PORE SATURATION MODEL FOR CAPILLARY IMBIBITION AND DRAINAGE PRESSURES

Dr. James E. Laurinat
Savannah River National Laboratory
Aiken, South Carolina

Abstract

Leaching and transport of radionuclides from cementitious waste forms and from waste tanks is a concern at the Savannah River Site and other Department of Energy sites. Computer models are used to predict the rate and direction for migration of these through the surrounding soil. These models commonly utilize relative permeability and capillary pressure correlations to calculate migration rates in the vadose (unsaturated) zone between the surface and the water table. The most commonly used capillary pressure models utilize two parameters to relate the pressure to the relative saturation between the wetting (liquid) and nonwetting (gas) phases. The correlation typically takes the form of a power law relation (e.g., Brooks and Corey and van Genuchten)[1,2] or an exponential equation (e.g., Kosugi).[3,4]

In this study, a pore saturation model is used to derive the capillary pressure as a function of a characteristic pore pressure and the wetting phase saturation. Singularity analyses of the total energies of the wetting and nonwetting phases give residual saturations for the two phases. The model includes separate pressures for imbibition and drainage to account for capillary hysteresis.

The model successfully correlates a selected set of laboratory imbibition and drainage data for sand, from the U. S. Salinity Laboratory's UNSODA database[5,6] and other sources.

The capillary pressure model utilizes a single fitting parameter, a characteristic pore pressure, which is related to a characteristic pore diameter by the Laplace equation. Data regression shows that this pore diameter approximately equals the diameter predicted from a capillary rise analysis based on the mean particle diameter.

Nomenclature

$\bar{d}_{part}$	volume average particle diameter for porous material
d_{pore}	effective pore diameter for porous material
G_s	potential energy associated with saturation of the porous medium
ΔG_{jump}	Gibbs free energy associated with jump condition between a homogeneous porous material and a porous material with fissures
H	molar enthalpy
k	Darcy coefficient for permeability
k_n	relative permeability to the nonwetting phase

k_w relative permeability to the wetting phase
n_i number of moles of the ith solute in the Gibbs' adsorption theorem calculation
P_a average pressure in the pores of the porous medium
P_c intrinsic capillary pore pressure, equal to the gas-liquid pressure difference
$P_{c,d}$ capillary pressure measured for drainage of the wetting phase
$P_{c,d,ms}$ capillary pressure measured for metastable drainage of the wetting phase
$P_{c,i}$ capillary pressure measured for imbibition of the wetting phase
$P_{c,i,0}$ minimum capillary pressure required to imbibe the wetting phase at the residual nonwetting phase saturation
$\Delta P_{c,ov}$ maximum reversible overshoot in the capillary pressure at the minimum saturation
P_{flow} characteristic pressure for flow in capillary pores
P_g gas phase pressure in capillary pores
ΔP_{jump} pressure change associated with jump condition between a homogeneous porous material and a porous material with fissures, applied to the liquid phase
P_l liquid phase pressure in capillary pores
P_{pot} potential pressure associated with partial saturation of capillary pores
$P_{v,i}$ vapor pressure of the ith solute in the Gibbs' adsorption theorem calculation
P_o ambient pressure for liquid in contact with the porous medium
R_g universal gas law constant
s relative saturation with the wetting phase
s^* saturation for a fissured soil, scaled so that it gives a capillary pressure equal to that of a nonfissured soil
s_{cr} critical saturation where the capillary pressure for imbibition equals the capillary pressure for drainage
s_{max} maximum saturation for a fissured porous material
s_{min} minimum saturation for a fissured porous material
s_{nr} residual nonwetting phase saturation
s_{wr} residual wetting phase saturation
T absolute temperature
v_n velocity of the nonwetting phase
v_w velocity of the wetting phase
W work required for flow through the porous medium
W_g work required for flow of gas through the porous medium
W_l work required for flow of liquid through the porous medium
z distance in the direction of flow
ε porosity

θ wetting angle
μ_n dynamic viscosity of the gas or nonwetting fluid
μ_w dynamic viscosity of the liquid or wetting fluid
σ air-water interfacial tension

Introduction

Capillary pressure represents the pressure required to displace a given volume of one of the phases from a two-phase mixture in a porous medium. The capillary pressure is typically measured either by imbibition or by drainage. Imbibition pressure measurements begin with uptake of liquid by the porous medium, typically a sand or soil, which initially is saturated with gas. For drainage pressure measurements, the gas displaces the liquid. (For convenience, this paper will refer to the terms wetting phase and liquid and nonwetting phase and gas interchangeably.)

During drainage, there exists a residual wetting saturation, s_{wr}, at which no additional amount of liquid can be displaced, no matter how much pressure is applied. For imbibition, as the liquid saturation increases, the imbibition pressure decreases. The pressure drops to zero, and absorption of liquid stops, at a maximum fractional wetting phase saturation, s_{nr}, called the residual nonwetting saturation. Significant drainage does not occur until a threshold pressure referred to as the displacement pressure or the entry head is exceeded. The drainage pressure then increases as the liquid saturation decreases. At any given saturation, the drainage capillary pressure exceeds the imbibition capillary pressure. The hysteresis between the two pressures is greatest at the residual nonwetting saturation.

Historically, the capillary pressure has been correlated as a function of the liquid saturation, normalized with respect to the difference between the residual nonwetting and wetting saturations. Most capillary pressure models utilize two parameters to relate the pressure to the relative saturation. The relationship typically takes the form of a power law relation (e.g., Brooks and Corey and van Genuchten),[1,2] an exponential equation (e.g., Kosugi),[3,4] or a combination of these two forms applied over different liquid saturation ranges (e.g., Rossi and Nimmo).[7] Brooks and Corey assigned the entry head, defined as the minimum capillary pressure during drainage, as one parameter and used the other parameter to characterize the pore size distribution. Several other models have followed this convention.

Parker and Lenhard[8] addressed the hysteresis between drainage and imbibition. They developed a model that includes effects of gas entrapment during imbibition. Their model defines limiting maximum capillary heads for drainage and minimum capillary heads for imbibition. They state that the actual pressure must lie at some value between these limits that depends on the flow history. A simple method of applying this model, applied by White and Oostrom,[9] is to define separate limiting capillary pressures for imbibition and drainage.

This paper presents a departure from traditional analytic models. A probabilistic pore pressure model and global energy balances replace the semi-empirical approach of

other models. The energy balances are solved for singularities in the driving forces for flow of the wetting and nonwetting phases, to obtain the residual wetting and nonwetting saturations, respectively. The pore pressure models are then used to calculate the capillary pressure as a function of saturation. Results are compared to selected capillary pressure measurements.

Derivation of Energy Balance for Capillary Pressure Model

The singularity analyses for the residual saturations are based on comparisons of the potential energy associated with the difference between the pressures of the two phases in the porous medium and the work required for flow of each phase. The analysis is loosely analogous to the Gibbs' adsorption theorem, which relates work done by surface forces to the chemical potential of a system. The model replaces the chemical potential with a mechanical potential based on the stored interfacial energy and substitutes a flow work term for the work needed to extend an interface. The model is applied to an adiabatic control volume within a larger volume of the porous medium, from which the only energy transfer occurs by flow of gas and liquid in or out. The model evaluates changes of the potential energy within the control volume and changes in the amount of flow work performed by the control volume on its surroundings.

The energy balance for the control volume takes the form

$$\Delta H = \Delta G_s + \Delta W \tag{1}$$

The energy balance is formulated in terms of the enthalpy because it is an open system in which liquid and gas may cross the volume boundaries.

Since the model assumes that the porous medium control volume is adiabatic, the enthalpy term is zero, and

$$\Delta G_s = -\Delta W \tag{2}$$

The mechanical potential and flow work terms can be expressed in terms of pressures much as the chemical potential in the Gibbs' adsorption equation. For a control volume initially comprised of one mole of gas, these expressions are

$$\Delta G_s = -R_g T \Delta ln\left(P_{pot}\right) \tag{3}$$

and

$$\Delta W = -R_g T \Delta\left(- ln\left(P_{flow}\right)\right) \tag{4}$$

The model employs different flow pressures for imbibition and drainage. The flow pressure for imbibition is based on liquid phase flow, while the flow pressure for drainage is based on gas phase flow.

Derivation of Pore Pressure Model

To derive the pressures for the potential energy and the flow work, a model for the pore pressure as a function of saturation must be developed. The pore pressure model assumes that each pore is filled with either a liquid wetting or a gaseous nonwetting phase. The capillary pore pressure is distributed by gas-liquid interfaces between the pores. The distribution of gas-and liquid-filled pores and the connections between pores are assumed to be random. The difference between the average pore pressure and the liquid pressure, according to this model, is equal to the product of the capillary pore pressure and the probability that a liquid-filled pore is in contact with a gas-filled pore and not with liquid in another pore. This probability, in turn, is the gas saturation. Thus, the difference between the average pore pressure and the liquid pressure is given by

$$P_a - P_l = P_c(1 - s) \tag{5}$$

Likewise, the difference between the gas pressure and the average pore pressure is equal to the product of the capillary pressure and the liquid saturation, or,

$$P_g - P_a = P_c s \tag{6}$$

The potential energy is calculated from the difference between the average pressure in the porous medium, P_a, and the reference pressure for flow through the porous medium, P_o. For an influx of liquid into the porous medium (imbibition), the reference pressure is the liquid phase pressure, and

$$P_a - P_o = P_c(1 - s) \tag{7}$$

For flow of gas (drainage), the reference pressure is the gas phase pressure, so that

$$P_a - P_o = -P_c s \tag{8}$$

These pressure differences apply only to the fractions of the pore volume occupied by liquid and gas, respectively. Consequently, for either liquid or gas flow, the potential energy is based on a pressure differential given by

$$P_{pot} = P_c s(1 - s) \tag{9}$$

The pressure differential is defined to be positive for both imbibition and drainage. Substitution of this pore pressure in the equation for the potential energy yields

$$\Delta G_s = -R_g T \Delta ln\left(P_c s\left(1-s\right)\right) \tag{10}$$

Analysis of Residual Saturations

At the residual wetting phase saturation, s_{wr}, the resistance to flow of the liquid becomes infinite, and, in an overall energy balance, the resistance to flow of the gas can be ignored. It may be stated, then, that for a given change in the saturation the change in the potential energy counteracts the change in the work needed to cause the liquid to flow. In other words, at $s = s_{wr}$,

$$\frac{dG_s}{ds} = -\frac{dW_l}{ds} \tag{11}$$

The liquid work function is derived from the Darcy equation for flow of two immiscible phases. The Darcy equation for the wetting phase is:

$$\varepsilon s v_w = -\frac{kk_w}{\mu_w}\frac{dP_l}{dz} = -\frac{kk_w}{\mu_w}P_c\frac{ds}{dz} \tag{12}$$

or

$$v_w = -\frac{kk_w}{\mu_w \varepsilon}P_c\frac{d\,ln\left(s\right)}{dz} \tag{13}$$

From this expression the pressure acting on a given volume of liquid is seen to be $P_c\,ln\left(s\right)$. The change in the corresponding work function is given by

$$\Delta W_l = -R_g T \Delta ln\left(-P_c\,ln\left(s\right)\right) \tag{14}$$

As with the potential energy, this expression gives the change in the work function for small changes in the saturation.

Substitution of this work term and the change in the potential energy in the energy balance yields

$$-R_g T\frac{d\,ln\left(P_c s\left(1-s\right)\right)}{ds} = -R_g T\frac{d\,ln\left(-P_c\,ln\left(s\right)\right)}{ds} \tag{15}$$

or

$$ln(s) = \frac{s-1}{1-2s} \tag{16}$$

This equation is satisfied for $s_{wr} = 0.236$.

A similar line of reasoning is used to calculate the residual saturation of the gas, s_{nr} . Here, the resistance to the gas flow is infinite, and the resistance to flow of the liquid can be ignored. Thus,

$$\frac{dG_s}{ds} = -\frac{dW_g}{ds} \tag{17}$$

The Darcy equation for the gas phase is:

$$\varepsilon(1-s)v_n = -\frac{kk_n}{\mu_n}\frac{dP_g}{dz} = -\frac{kk_n}{\mu_n}P_c\frac{ds}{dz} \tag{18}$$

or

$$v_n = -\frac{kk_n}{\mu_n \varepsilon}\left(-P_c\frac{d\,ln(1-s)}{dz}\right) \tag{19}$$

From this expression the pressure acting on a given volume of gas is seen to be $-P_c\,ln(1-s)$. The capillary pressure is subtracted from this pressure. The capillary pressure is supplied to the gas to convert it from a stationary state in which it is in contact with a pore wall to a mobile state in which it is surrounded by liquid. The total pressure supplied to the gas phase is, therefore, $-P_c(1+ln(1-s))$, and the corresponding change in the work function is:

$$\Delta W_g = -R_g T \Delta\, ln(-P_c(1+ln(1-s))) \tag{20}$$

Substitution of this work term and the change in the potential energy in the energy balance gives

$$-R_g T\frac{d\,ln(P_c s(1-s))}{ds} = -R_g T\frac{d\,ln(-P_c(1+ln(1-s)))}{ds} \tag{21}$$

or

$$ln(1-s)=\frac{3s-1}{1-2s} \tag{22}$$

This equality is satisfied for $s_{nr}=0.884$.

Measured residual saturations for a uniform sand[10,11,12] agree almost exactly with the derived values; the measured wetting saturation, estimated by graphical interpolation, was 0.230, and the measure wetting saturation was 0.884.

Calculation of Capillary Pressures for Imbibition and Drainage

The following section describes a capillary pressure model for imbibition and drainage, based on the residual nonwetting saturation. For imbibition, the wetting phase, or liquid, supplies the motive force for displacement of the nonwetting, or gas, phase. Consequently, it may be argued that the effective capillary pressure within the porous medium is the integral of the pressure gradient for the liquid phase. During imbibition, the force to displace the gas is applied over the entire surface of the porous medium, but the medium can be considered to be aerated so that the air within the capillary pores remains at atmospheric pressure. A hydraulic advantage accompanies the force applied to the liquid in the pores, then, in inverse proportion to the liquid saturation. It follows that the measured liquid pressure is the integral of the liquid phase pressure gradient, divided by the saturation. This gives for the measured capillary pressure for imbibition:

$$\frac{P_{c,i}}{P_c}=\frac{P_{c,i,0}}{P_c}-\frac{ln(s)}{s} \tag{23}$$

where $P_{c,i,0}$ represents the minimum pressure required for imbibition of liquid into a saturated porous medium containing non-displaceable gas.

During drainage, both liquid and gas displace the liquid that leaves the porous medium. Hence it may be argued that the effective capillary pressure is the volume average of the integrals of the pressure gradients for the gas and the liquid. Again, because the air remained at atmospheric pressure during drainage, there is a hydraulic advantage applied to the measured pressure, so the effective pressure is this volume-average pressure integral, divided by the saturation.

At the maximum residual nonwetting phase saturation, the measured suction pressure drops by a step change from its value for drainage to its value for imbibition. This pressure change can be attributed to the change from a continuous gas phase at atmospheric pressure to a continuous liquid phase for which, at static equilibrium, the outside pressure equals the liquid phase pressure. Since the liquid phase pressure is less than the gas phase pressure by the characteristic capillary pore pressure, the

suction pressure for imbibition must be less than the pressure for drainage by just this pressure, divided by the saturation to account for the effective hydraulic advantage. These considerations, with adjustments to account for differences between the integration constants for the liquid and volume-average pressure gradients, give, for the capillary pressure for drainage,

$$\frac{P_{c,d}}{P_c} = \frac{P_{c,i,0}}{P_c} + \frac{1}{s_{nr}} - \frac{ln(s_{nr})}{s_{nr}} + \frac{(1-s)[1+ln(1-s)] - s\,ln(s)}{s} \tag{24}$$

$$- \frac{(1-s_{nr})[1+ln(1-s_{nr})] - s_{nr}\,ln(s_{nr})}{s_{nr}}$$

The minimum suction pressure required for imbibition into a liquid-saturated porous medium, i.e., the entry head, most likely is a function of the capillary pore pressure. The most plausible explanation that fits the measured data is that an excess capillary force is required to displace air from an array of pores located on the surface in all three directions (one perpendicular to the surface and two in transverse directions). The required force is the three-dimensional vector sum of the forces required for unidirectional displacement, one component of which corresponds to the pressure. According to this interpretation, the minimum capillary pressure is the pore pressure multiplied by the square root of three:

$$\frac{P_{c,i,0}}{P_c} = \sqrt{3} \tag{25}$$

This entry head is applied at the outer surface of the porous medium, so this pressure difference is not normalized with respect to the liquid saturation.

A combination of the capillary pressure equations for imbibition and drainage yields a critical saturation where these two pressures coincide:

$$\frac{1-(1-s_{nr})[1+ln(s_{nr})+ln(1-s_{nr})]}{s_{nr}} = -\frac{(1-s_{cr})[1+ln(s_{cr})+ln(1-s_{cr})]}{s_{cr}} \tag{26}$$

Substitution of s_{nr} in this expression gives $s_{cr} = 0.301$.

Below this saturation, the suction pressure that develops during drainage is less than the suction pressure that accompanies imbibition. The logical conclusion is that the porous medium will not drain to a saturation below this critical value, unless the source of liquid is removed from contact with the porous medium or there is an external gas flow.

Comparison of Model Predictions to Capillary Pressure Data

Data from the UNSODA database maintained by the George E. Brown, Jr., Salinity Laboratory of the U. S. Department of Agriculture,[5,6] was selected for comparison with the model. The comparison is limited to data sets with paired imbibition and drainage pressures that exhibited a significant entry head $P_{c,i,0}$ and that included particle size measurements. There were three such data sources, namely Shen and Jaynes,[13] Stauffer and Dracos,[14] and Poulosavassilis.[15] An additional data source not included in the UNSODA data base, that of Smiles et al. and Vachaud and Thony,[16,17] also is analyzed. All of these data sources contained measurements made in sand. The fitting procedure entailed a calculation of the capillary pore pressure P_c, computed as the average of the measured capillary pressures divided by the capillary pressures predicted by the model at the relative saturations for each measurement. To eliminate measurements near saturation with either liquid or gas, the calculation was limited to relative liquid saturations between 0.4 and 0.75.

Figure 1 compares these data with model predictions. As this figure shows, the Shen and Jaynes data and the Stauffer and Dracos data have minimum measured saturations about half the predicted critical minimum saturation s_{cr}, while the Poulovassilis and Smiles et al. data have minimum measured saturations approximately equal to s_{cr}.

The model fits the data closely for the Poulovassilis and Smiles et al. data. The most logical explanation for the apparent discrepancy between the minimum measured saturations for the Shen and Jaynes and the Stauffer and Dracos data and the model prediction is that the porous material develops fissures that fill with gas during drainage. According to this interpretation, the fissures are larger than the pores by a sufficient magnitude that they do not offer any flow resistance but rather simply conduct fluid among the pores. The minimum saturation for a fissured material can be derived by applying a jump condition for the development of fissures. Following the logic used in the analysis of residual wetting saturations, the pressure applied to the liquid phase across such a jump, ΔP_{jump}, is

$$\Delta P_{jump} = P_c\left[\left(1 - s_{min}\right) - \left(1 - s_{cr}\right)\right] = P_c\left(s_{cr} - s_{min}\right) \tag{27}$$

The minimum saturation is the saturation that will minimize the free energy associated with this jump, ΔG_{jump}. This free energy, evaluated after the appearance of the fissures, is

$$\Delta G_{jump} = -R_g T\, ln\left(P_c s_{min}\left(s_{cr} - s_{min}\right)\right) \tag{28}$$

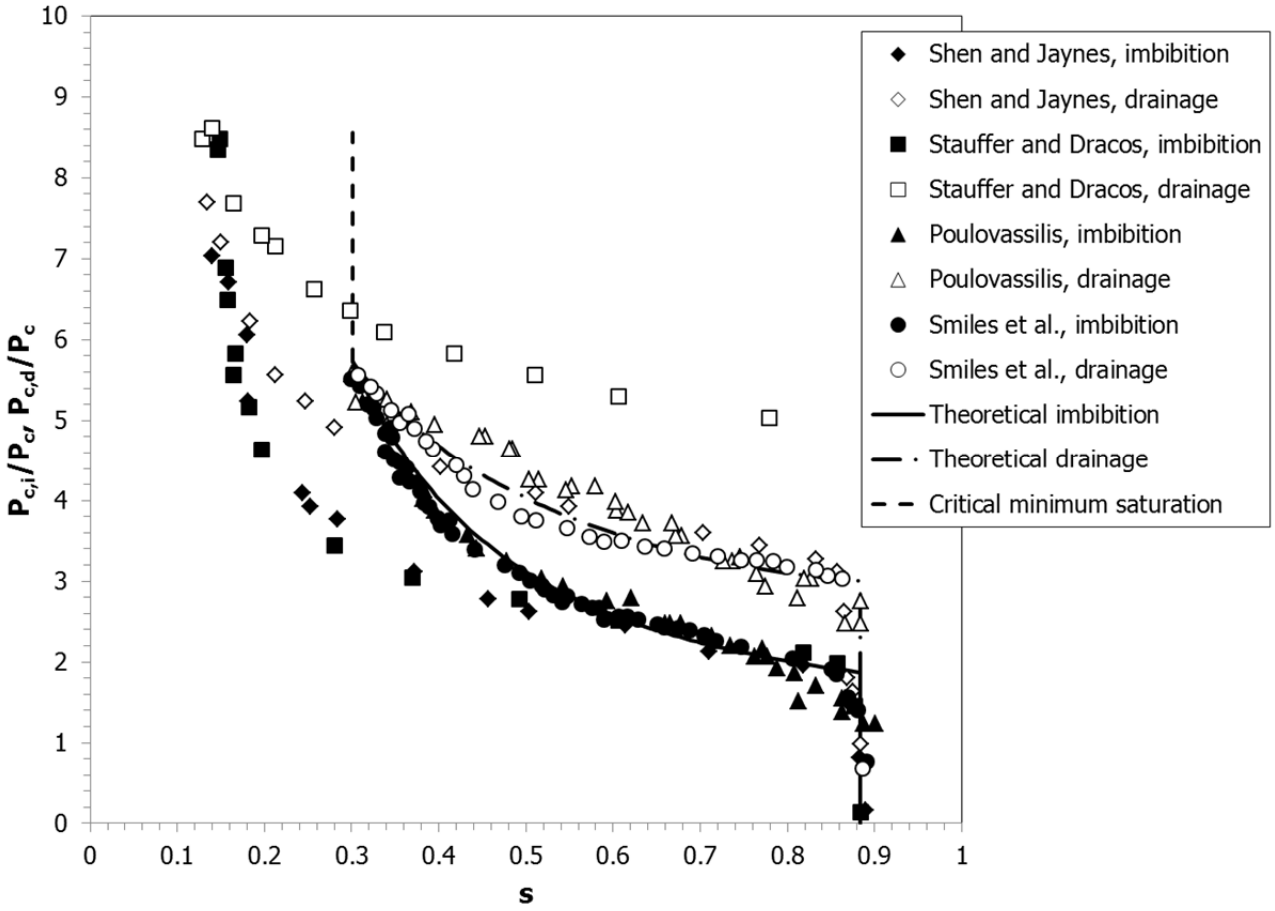

Figure 1. Variation of Imbibition and Drainage Pressures with Relative Saturation

This condition is satisfied by

$$s_{min} = 0.5\, s_{cr} \tag{29}$$

A similar analysis, combined with the observation that the maximum saturation for a homogeneous porous material is the residual nonwetting saturation, gives for the maximum saturation for a fissured porous medium s_{max},

$$s_{max} = 0.5 + 0.5\, s_{rn} \tag{30}$$

The capillary pressure model describes the saturation for just the pores of a fissured material. Because the fissure volume merely conducts pressure among the pores, the overall saturation for the total volume of porous material is a linear function of the pore saturation. If the maximum saturation is defined to be equal to the residual nonwetting saturation to conform with the model, then a linear interpolation between

this saturation and the minimum saturation yields the following expression for the overall saturation of a fissured material, s^*, as a function of the model saturation for a homogeneous porous material, s, the residual nonwetting saturation, s_{nr}, and the critical saturation, s_{cr}:

$$s^* = \frac{0.5\, s_{cr}\, s_{nr} - s_{cr}\, s + s_{nr}\, s}{s_{nr} - 0.5\, s_{cr}} \tag{31}$$

Figure 2 compares the capillary pressure model with the Shen and Jaynes data and the Stauffer and Dracos data defined by s^*. The model fits the adjusted imbibition data closely, but the Stauffer and Dracos drainage data deviate significantly from the model. The difference between the measured and predicted drainage pressures remains approximately constant as the saturation increases. This suggests the presence of a metastable equilibrium that originates from the upstream (dry) side of the capillary pressure gradient.

The most plausible explanation for the overshoot and apparent metastability phenomena is that at the minimum liquid saturation, the interstitial gas in the fissures begins to exert pressure on the residual liquid in the pores. As explained in the capillary pressure model derivation, this pressure would be the product of the capillary pore pressure P_c and the fraction of the volume occupied by the interstitial gas, $0.5\left(1 - 0.5\, s_{cr}\right)$, divided by the residual pore saturation, $0.5\, s_{cr}$. Thus, the overshoot pressure $\Delta P_{c,ov}$ is given by

$$\frac{\Delta P_{c,ov}}{P_c} = \frac{1 - 0.5\, s_{cr}}{s_{cr}} \tag{32}$$

The apparent metastability, according to this interpretation, results when the overshoot in the capillary pressure at minimum saturation propagates downstream in the nonwetting (gas) phase. The fraction of the overshoot pressure that propagates would be equal to the fraction of the pore volume occupied by gas, $1 - s_{cr}$. If this overshoot pressure propagates, then the metastable drainage pressure $P_{c,d,ms}$ would be given by

$$\frac{P_{c,d,ms}}{P_c} = \frac{P_{c,d}}{P_c} + \frac{\left(1 - s_{cr}\right)\left(1 - 0.5\, s_{cr}\right)}{s_{cr}} \tag{33}$$

As shown by Figure 2, the predicted overshoot pressure approximately equals maximum measured pressures, and the Stauffer and Dracos data closely follow the predicted metastable drainage pressure curve.

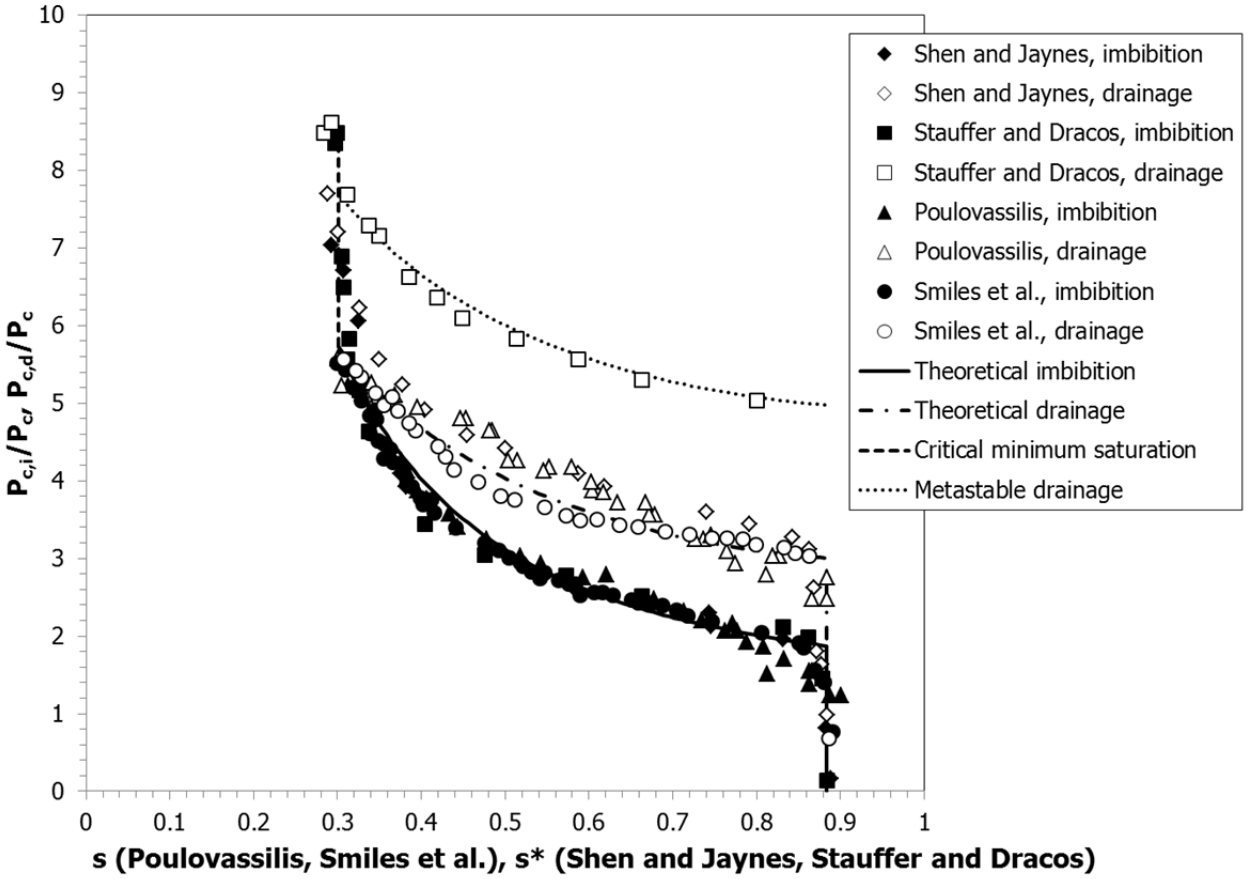

Figure 2. Variation of Imbibition and Drainage Pressures with Relative Saturation, Corrected for Fissure Effect

Evaluation of Characteristic Pore Pressures

The final step in development of the capillary pressure model is to relate the characteristic pore pressure P_c derived from the data fit to the particle size of the porous material. (One may recall that, for each data set that was regressed, the pressure multiplier is $\frac{1}{P_c}$.) From an analysis of the capillary rise in a powder, based on the specific surface area of the powder, Dunstan and White derived the following relationship between the average particle diameter and the pore diameter:[18,19]

$$d_{pore} = \frac{2\varepsilon}{3(1-\varepsilon)}\bar{d}_{part} \tag{34}$$

Average particle diameters were calculated from sieve tray data using an interval-censored method[20] based on an assumed log normal size distribution. For each data set, the void fraction was either given, calculated from the bulk density of the

sand, or estimated by fitting the residual nonwetting saturation to the capillary pressure data.

The pore diameter also is related to the interfacial tension, σ, the liquid wetting angle, θ, and the capillary rise pressure, $P_{c,i,0}$, by the Laplace relation:

$$d_{pore} = \frac{4\sigma cos(\theta)}{P_{c,i,0}} \tag{35}$$

The surface tension of water at room temperature is 72.2 dyne/cm^2.[21] The measured wetting angle is highly variable and depends on the measurement method. For air-dried sand, a dynamic measurement method angle yields a wetting angle of 45°.[22]

Table 1 compares pore diameters calculated from the average particle diameter (Equation 34) and the capillary rise pressure to the characteristic pore diameter for the capillary pressure model presented in this study (Equation 35). As may be seen, these pore diameters are in relatively close agreement; the pore diameter calculated from the capillary pressure model differs from the pore diameter calculated from the average particle diameter by an average of 7%, with a standard deviation of ±25%.

Table 1. Comparison of Pore Diameters from Particle Diameter and Capillary Pressure Measurements

Data Set	$\bar{d}_{part}$, μm	d_{pore} from $\bar{d}_{part}$, μm	d_{pore} from $P_{c,i,0}$, μm	Deviation, %
Shen and Jaynes	354	200	160	-20
Stauffer and Dracos	312	167	135	-19
Poulovassilas	537	185	219	18
Poulovassilas	551	154	205	33
Smiles et al.	264	100	122	23

Conclusions

A model has been developed that uses a characteristic pore pressure to predict residual wetting and nonwetting saturations and capillary imbibition and drainage pressures. The model is based on an energy balance that equates changes in potential surface energy to changes in pressure-volume work. A simple probabilistic distribution expresses capillary forces as a function of the relative saturation and the characteristic pore pressure. The model implicitly assumes that the porous medium is homogeneous and isotropic.

The model predicts a residual wetting saturation, s_{wr}, of 0.236 and a residual nonwetting saturation, s_{nr}, of 0.884. These predicted residual saturations are in

almost exact agreement with measurements. In addition, the model predicts that there is a critical saturation, s_{cr}, of 0.301, below which the imbibition pressure exceeds the drainage pressure. A porous medium will not drain to any lower saturation, provided that the porous medium remains in contact with liquid and there is no external gas flow.

The capillary pressure model successfully correlates limiting imbibition and drainage pressures for selected laboratory tests that used uniformly packed, sieved sand, although for certain tests an adjusted saturation is required to account for fissures. For the data that was correlated, the characteristic pore diameter from the capillary pressure model approximately equals the pore diameter calculated from the average particle diameter using a capillary rise model. This agreement suggests that, for uniform packed sands with a relatively narrow particle size distribution, a capillary pressure curve can be estimated from a measured particle size distribution. The applicability of the model to soils and rocks with widely varying pore size distributions has not been demonstrated.

Acknowledgment

This work was funded by the U. S. Department of Energy Office of Environmental Management under contract number DE-AC09-08SR22470.

References

1. Brooks, R.H. and A.T. Corey (1964), “Hydraulic properties of porous media,” Hydrol. Pap. 3, Civ. Eng. Dept., Colorado State University, Fort Collins, Colo.
2. van Genuchten, M.T. (1980), “A closed-form equation for predicting the hydraulic conductivity of unsaturated soils,” Soil Sci. Soc. Am. J. 44, 892-898.
3. Kosugi, K. (1994), “Three-parameter lognormal distribution model for soil water retention,” Water Resour. Res. 30(4), 891-901.
4. Kosugi, K. (1996), “Lognormal distribution model for unsaturated soil hydraulic properties,” Water Resour. Res. 32(9), 2697-2703.
5. Nemes, A., M.G. Schaap, and F.J. Leij (1999), “The UNSODA unsaturated soil hydraulic database, version 2.0,” U. S. Salinity Laboratory, U. S. Department of Agriculture, Agricultural Research Service, Riverside, California.
6. Nemes, A., M.G. Schaap, F.J. Leij, and J.H.M. Wosten (2001), “Description of the unsaturated soil hydraulic database UNSODA version 2.0,” J. Hydrol. 251(3-4), 151-162.
7. Rossi, C. and J.R. Nimmo (1994), “Modeling of soil water retention from saturation to oven dryness,” Water Resour. Res. 30(3), 701-708.
8. Parker, J.C. and R.J. Lenhard (1987), “A model for hysteric constitutive relations governing multiphase flow: 1. Saturation-pressure relations,” Water Resour. Res. 23(12), 2187-2196.

9. White, M.D. and M. Oostrom (1996), "STOMP, subsurface transport over multiple phases: theory guide," U.S. DOE Pacific Northwest National Laboratory Report PNNL-11217, UC-2010.
10. Demond, A.H. and P.V. Roberts (1991), "Effect of interfacial forces on two-phase capillary pressure-saturation relationships," Water Resour. Res. 27(3), 423-437.
11. Morel-Seytoux, H.J. and J. Khanji (1975), "Prediction of imbibition in a horizontal column," Soil Sci. Soc. Am. Proc. 39, 613-617.
12. Morel-Seytoux, H.J., J. Khanji, and G. Vachaud (1973), "Prediction errors due to uncertainties in the measurement and extrapolation of the diffusivity function," Civil Engineering Report, Colorado State University, Fort Collins, Colorado 80523, CEP72-73, HJM48.
13. Shen, R. and D.B. Jaynes, (1988), "Effect of soil water hysteresis on simulation, infiltration, and distribution," Shuili Xuebao: J. Hydr. Eng. (China) 10, 11-20.
14. Stauffer, F. and T. Dracos (1986), "Experimental and numerical study of water and solute infiltration in layered porous media," J. Hydrol. 84(1-2), 9-34.
15. Poulovassilis, A. (1970), "Hysteresis of pore water in granular porous bodies," Soil Sci. 109(1), 5-12.
16. Smiles, D.E., G. Vachaud, and M. Vauclin (1971), "A test of the uniqueness of the soil moisture characteristic during transient, nonhysteric, flow of water in a rigid soil," Soil Sci. Soc. Am. Proc. 35, 534-539.
17. Vachaud, G. and J.-L. Thony (1971), "Hysteresis during infiltration and redistribution in a soil column at different initial water contents," Water Resour. Res. 7(1), 111-127.
18. White, L.R. (1982), "Capillary rise in powders," J. Colloid Interf. Sci. 90(2), 536-538.
19. Dunstan, D., and L.R. White (1986), "A capillary pressure method for measurement of contact angles in powders and porous media," J. Colloid Interf. Sci. 111(1), 60-64.
20. So, Y., G. Johnston, and S.H. Kim, "Analyzing Interval-Censored Data with SAS® Software," Paper 257-2010, Proceedings, SAS Global Forum 2010, Seattle, Washington, April 11-14, 2010.
21. Lide, D.R., ed. (1994), CRC Handbook of Chemistry and Physics, 75th ed., CRC Press, Boca Raton, Florida.
22. Weisbrod, N., T. McGinnis, M.L. Rockhold, M.R. Niemet, and J.S. Selker (2009), "Effective Darcy-scale contact angles in porous media imbibing solutions of various surface tensions," Water Resour. Res. 45(4), W00D39.